Inorganic Chemistry

Article

pubs.acs.org/IC

Redox Potential Determines the Reaction Mechanism of HNO Donors with Mn and Fe Porphyrins: Defining the Better Traps

Lucía Álvarez,[†] Sebastián A. Suarez,[†] Damian E. Bikiel,[†] Julio S. Reboucas,[§] Ines Batinić-Haberle,[∥] Marcelo A. Martí,[†,‡] and Fabio Doctorovich*[,†]

[†]Departamento de Química Inorgánica, Analítica y Química Física, Facultad de Ciencias Exactas y Naturales, INQUIMAE-CONICET and [‡]Departamento de Química Biológica, Facultad de Ciencias Exactas y Naturales, Universidad de Buenos Aires, Ciudad Universitaria, Pab. II (1428), Buenos Aires, Argentina

[§]Departamento de Quimica, CCEN, Universidade Federal da Paraiba, Joao Pessoa, Paraiba, Brazil

[∥]Department of Radiation Oncology, Duke University Medical School, Durham, North Carolina 27710, United States

Supporting Information

ABSTRACT: Azanone (^{1}HNO, nitroxyl) is a highly reactive molecule with interesting chemical and biological properties. Like nitric oxide (NO), its main biologically related targets are oxygen, thiols, and metalloproteins, particularly heme proteins. As HNO dimerizes with a rate constant between 10^6 and 10^7 M^{-1} s^{-1}, reactive studies are performed using donors, which are compounds that spontaneously release HNO in solution. In the present work, we studied the reaction mechanism and kinetics of two azanone donors Angelís Salt and toluene sulfohydroxamic acid (TSHA) with eight different Mn porphyrins as trapping agents. These porphyrins differ in their total peripheral charge (positively or negatively charged) and in their Mn^{III}/Mn^{II} reduction potential, showing for each case positive (oxidizing) and negative (reducing) values. Our results show that the reduction potential determines the azanone donor reaction mechanism. While oxidizing porphyrins accelerate decomposition of the donor, reducing porphyrins react with free HNO. Our results also shed light into the donor decomposition mechanism using ab initio methods and provide a thorough analysis of which MnP are the best candidates for azanone trapping and quantification experiments.

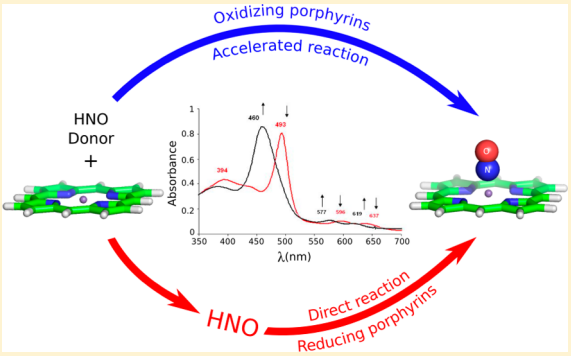

INTRODUCTION

Azanone (^{1}HNO, nitroxyl) is a highly reactive molecule with interesting chemical and biological properties.[1,2] Like its "elder brother" nitric oxide (NO), its main biologically related targets are oxygen, thiols, and metalloproteins, particularly heme proteins.[1] One of the most important features related to HNO chemistry lies in the fact that it reacts with itself (i.e., it dimerizes) to yield nitrous oxide and water with a rate constant between 10^6 and 10^7 M^{-1} s^{-1}.[3] For this reason, azanone chemical reactivity or biological effect studies must rely on the use of donors, such as trioxodinitrate (Angeli's Salt, AS) or toluene sulfohydroxamic acid (TSHA), both of which among others have been shown to produce distinct pharmacological effects when compared to NO donors.[2,4,5] Also, for this same reason its detection and quantization relies mainly on the use of trapping agents, which react with free HNO and yield a product that is later detected with some spectroscopic and/or analytical method. The relevance of nitroxyl arises from studies that invoke its presence as a key intermediate species in several interesting chemical reactions.[6−12] Its significance is also supported by results indicating that it could act as a physiological signaling molecule (like NO) that would be enzymatically produced under particular circumstances by nitric oxide synthase or other biologically related reactions.[13] Confirmation of these hypotheses, however, requires strict confirmation through unequivocal determination of its presence, which underscores the relevance of the development of HNO-selective sensing devices.

HNO and NO Reactivity with Metalloporphyrins. Metalloporphyrins have been widely used as chemical models of heme proteins, providing us with invaluable tools for the study of small molecules, like NO or O_2, coordination chemistry, and metal-catalyzed reactions. Many studies with iron, manganese, cobalt, and also other transition metal porphyrins have been performed showing diverse mechanistic, kinetic, structural, and reactive aspects related to formation of nitrosyl complexes.[14−17] Porphyrins are also widely used in technical applications, especially when coupled to a surface, where they can be used as electrochemical gas sensors.[18] Thus, and given their reduction potential, they are key players in azanone chemical biology studies. Key to our understanding of

Received: March 26, 2014
Published: July 8, 2014

   dx.doi.org/10.1021/ic5007082 | Inorg. Chem. 2014, 53, 7351−7360

metalloporphyrin nitrosyl complexes are their NO−ligand association (k_{on}) and dissociation rates constants (k_{off}) as well as the electronic structure and structural characteristics of the adduct.[19] Usually NO binds to the metal via the nitrogen atom, and its character ranges (formally) from that of NO^+ to that of NO^-. (To describe porphyrin nitrosyl complex characteristics in a general way the Enemark and Feltham notation is used, where the metal−NO complexes are described as $\{MNO\}^n$ complexes, where M is the corresponding metal center and the key parameter is the number n, corresponding to the sum of the metal d electrons plus the nitrosyl π^* electrons.) A key breakthrough in the complex chemistry of azanone with porphyrins was established about 10 years ago by Farmer and co-workers, where it was proven that ferrous myoglobin ($Fe^{II}Mb$) was able to form a stable Fe^{II}−HNO adduct, thus the first $\{Fe(H)NO\}^8$ complex.[20−22] Around that time, we found that metalloporphyrins are efficient HNO traps.[17,23] A few years later, our group showed that by the use of electron-withdrawing synthetic iron porphyrins it is possible to stabilize $\{FeNO\}^8$ species which show, as expected, electronic structure characteristics of an NO^- (nitroxyl) adduct.[24] More recently, Lehnert and co-workers obtained spectroscopic evidence for formation of an HNO picket-fence porphyrin.[25] Manganese porphyrins have also been shown to form stable nitrosyl $\{MnNO\}^6$ complexes with a linear Mn−N−O geometry, while cobalt porphyrins show highly stable $\{CoNO\}^8$ and less stable $\{CoNO\}^7$ adducts.[16,17]

Reaction Kinetics. Most of our understanding of the kinetics of nitrosyl complexes comes from studies with iron porphyrins. NO displays fast (ca. 10^6 M^{-1} s^{-1}) and very fast (ca. 10^9 M^{-1} s^{-1}) association rates constants with ferric and ferrous porphyrins, respectively.[26] This difference is probably due to the fact that in ferric porphyrins a water molecule or hydroxide ion needs to be displaced prior to NO binding. Nitric oxide dissociation rates constants are, on the other hand, moderate (1−500 s^{-1}) for ferric $\{FeNO\}^6$ and very small (<1 × 10^{-4} s^{-1}) for ferrous $\{FeNO\}^7$ complexes, which results in their huge differential stability. A similar trend is observed in heme proteins. Azanone association to ferrous porphyrins has not been reported since $\{FeHNO\}^8$ complexes are not stable in isolated porphyrins, except for the recently reported picket-fence HNO porphyrin.[25] In the case of ferrous Mb, the rate constant has been reported to be ca. 1 × 10^4 M^{-1} s^{-1}.[27] Interestingly and as shown in previous works from our group, Fe(III) and Mn(III) porphyrins are able to react efficiently with azanone donors to yield the stable $\{FeNO\}^7$ and $\{MnNO\}^7$ complexes with rate constants estimated to be ca. 1 × 10^5 M^{-1} s^{-1}.[17,23,28,29] However, as will be described below, reaction of metalloporphyrins with azanone donors follow a complex mechanism.

Putative Reaction Mechanisms of HNO Donors with Mn^{III} and Fe^{III} Porphyrins. The first and striking observation for reactions of azanone donors with Mn^{III} and Fe^{III} porphyrins is that the effective $\{MNO\}^7$ product formation rate and stoichiometric donor/porphyrin ratio needed to achieve total conversion displays two radically different behaviors, which in our previous works[28] was related to the porphyrin peripheral charge. We observed that for negatively charged porphyrins such as $[Fe^{III}TSPP]^{3-}$ and $[Mn^{III}TSPP]^{3-}$ the reaction with AS at pH 7 (where AS spontaneous decomposition has a half-life of about 900 s at room temperature) required a large excess of AS to drive the reaction to completion and for an equimolar ratio the reaction half-life was ca. 120 min.[17,28] On the other hand, reaction of positively charged porphyrins such as $[Fe^{III}TE\text{-}2\text{-}PyP]^{5+}$ and $[Mn^{III}TE\text{-}2\text{-}PyP]^{5+}$ showed total conversion to the nitrosyl metalloporphyrin, with an equimolar porphyrin to donor ratio, in less than 10 s.[17,28] A similar behavior was observed for reactions with the azanone donor TSHA. The fact that the overall reaction rate for positively charged porphyrins by far exceeds the donor spontaneous decomposition rate and that the reaction is first order in donor concentration strongly suggested that in those cases a direct porphyrin−donor interaction was taking place and that those porphyrins accelerate donor decomposition. For the negatively charged porphyrins, where the reactions were slower and the plot of observed rate vs donor concentration is not linear, the expected spontaneous HNO generation by the donor and subsequent azanone reaction with the porphyrin was assumed to be the operative mechanism. Both mechanisms are presented in Scheme 1, where $k_{on(Donor)}$ represents the bimolecular

Scheme 1. Reaction Mechanisms between Metalloporphyrin and HNO Donors

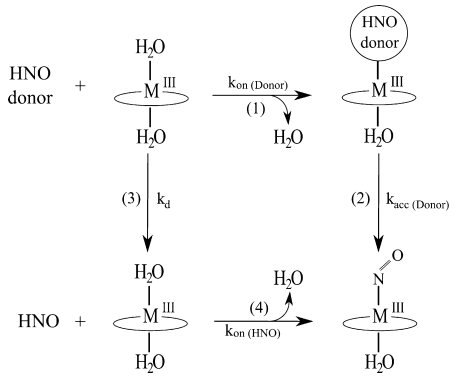

association rate constant of the metalloporphyrin with the HNO donor, $k_{acc(Donor)}$ represents the porphyrin-accelerated donor decomposition rate constant, k_d represents the spontaneous donor decomposition rate constant to yield HNO, and $k_{on(HNO)}$ is the bimolecular metalloporphyrin-to-HNO association rate, associated with MP trapping of azanone. This scheme allows determination of the corresponding key rate constants for both limiting cases, $k_{on(Donor)}$ and $k_{on(HNO)}$, although little is known about the reasons underlying the observed differences. Understanding the molecular basis of the azanone donor−porphyrin reactions is important both to the use of porphyrins as HNO trapping-quantification agents and for understanding how is HNO liberated by the donor.

In the present work, we studied the reaction mechanism and kinetics of two azanone donors AS and TSHA with eight different Mn porphyrins (see below) that differ systematically in their total peripheral charge (positively or negatively charged) and in their Mn^{III}/Mn^{II} reduction potential, showing for each case positive (oxidizing) and negative (reducing) values. Our results show that the reduction potential is key for determining the donor−metalloporphyrin reaction mechanism, shed light into the donor decomposition mechanism, and provide a thorough analysis of which $Mn^{III}P$ are the best candidates for azanone trapping and quantification experiments.

MATERIALS AND METHODS

Reagents. Angeli's salt (trioxodinitrate, $N_2O_3^{2-}$, AS) and *N*-hydroxy-4-methylbenzenesulfonamide (TSHA) were synthesized according to published literature procedures.[30,31] Manganese(III)

dx.doi.org/10.1021/ic5007082 | Inorg. Chem. 2014, 53, 7351−7360

Scheme 2. Chemical Structures of the Mn/Fe Porphyrins Used in the Present and Previous Works[17,23,28a]

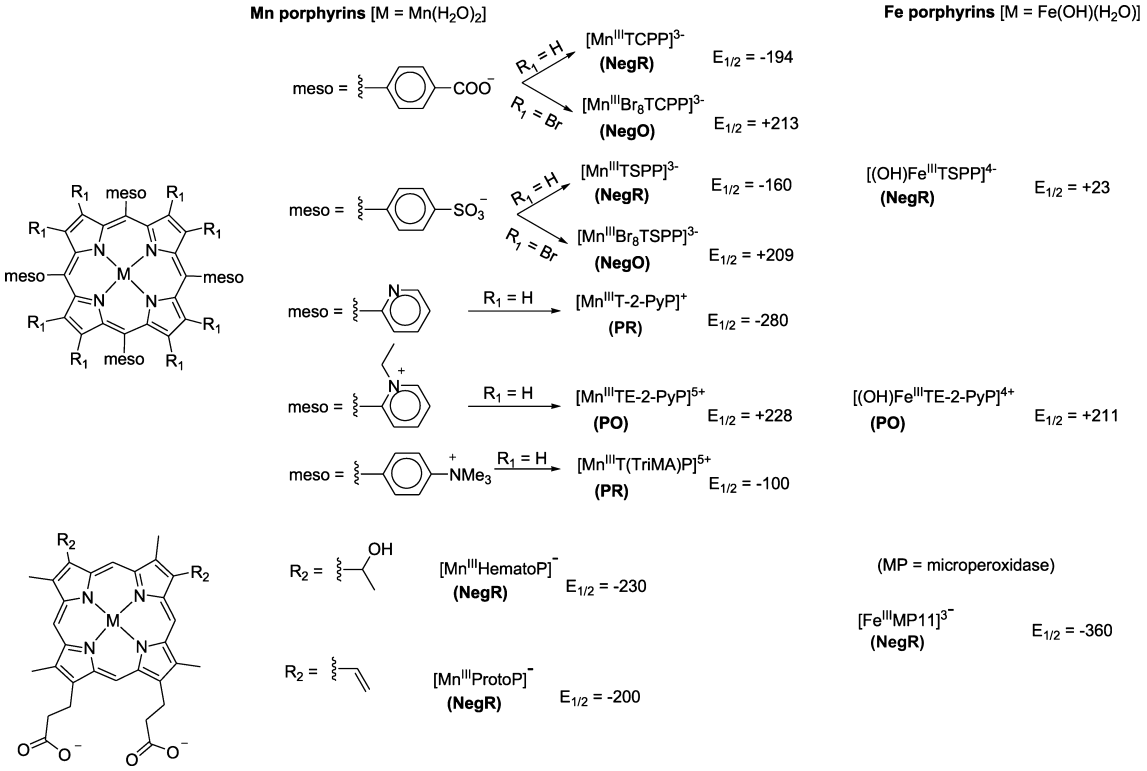

[a]Reduction potential ($E_{1/2}$) corresponds to the M^{II}/M^{III} couple vs NHE and is reported in mV.[34]

meso-tetrakis(4-sulfonatophenyl)porphyrin ($[Mn^{III}TSPP]^{3-}$) and manganese(III) *meso*-tetrakis(*N*-ethylpyridinium-2-yl)porphyrin ($[Mn^{III}TE\text{-}2\text{-}PyP]^{5+}$) were purchased from Frontier Scientific. Mn(III) *meso*-tetrakis(*p*-carboxylatophenyl)porphyrin ($[Mn^{III}TCPP]^{3-}$), Mn(III) *β*-octabromo-*meso*-tetrakis(4-carboxylatophenyl)porphyrin ($[Mn^{III}Br_8TCPP]^{3-}$), Mn(III) *β*-octabromo-*meso*-tetrakis(4-sulfonatophenyl)porphyrin ($[Mn^{III}Br_8TSPP]^{3-}$), Mn(III) hematoporphyrin-IX ($[Mn^{III}HematoP]^{-}$), Mn(III) protoporphyrin-IX ($[Mn^{III}ProtoP]^{-}$), Mn(III) *meso*-tetrakis(4-*N*,*N*,*N*-trimethylanilinium)porphyrin $[Mn^{III}T(TriMA)P]^{5+}$, and Mn(III) *meso*-tetrakis(2-pyridyl)porphyrin ($[Mn^{III}T\text{-}2\text{-}PyP]^{+}$) were synthesized pure as described in previous works.[32−37]

Reactions of Metalloporphyins with HNO Donors. The overall strategy used to measure HNO reactions with different porphyrins is the same as that reported in our previous works on the subject[1,17,23] and will be described briefly. All experiments were done at 25 °C in 0.1 M phosphate buffer containing 10^{-4} M EDTA to avoid donor and/or HNO catalytic decomposition by Cu^{II} and other divalent ions. Porphyrin concentrations were ca. 8×10^{-6} M, unless otherwise noted. UV−vis spectra were recorded with a HP 8453 spectrometer in a septum-sealed 1 cm path quartz cell. All manipulations were performed under argon atmosphere. AS and TSHA solutions were freshly prepared for each set of measurements and kept on ice, and the donor concentration was checked before each measurement by following the corresponding absorbance.[38−40] TSHA was dissolved in ethanol 96% and added to the porphyrin solutions to a final ethanol/water ratio of less than 1%. Reactions were monitored by following the absorbance of the porphyrins at the peak position of the Soret and/or Q bands.

Determination of the Rate Constants. The overall strategy used to determine the rate constants is the same as that reported in our previous works on the subject[1,17,23] and will be only described briefly. Observed initial reaction rates of nitrosyl product formation (d[PNO]/d*t* or simply v_{on}) were determined using standard fitting procedures from the absorbance vs time plots at the Soret and/or Q-band peak position, which reflect formation of the nitrosylporphyrin and free porphyrin decay. All reactions were pursued until no more spectroscopic changes were observed, unless otherwise stated. Reaction times ranged from 60 s to 1 h for different stoichiometric donor/porphyrins ratios and different porphyrins. Kinetic data analysis was subsequently performed according to each of the presented mechanisms shown in Scheme 1. In those cases where the reaction is suspected to occur through direct donor−porphyrin interaction, $k_{on(Donor)}$ was determined from the corresponding v_{on} vs donor concentration plots, corresponding to the following reaction rate law

$$v_{on} = k_{on(Donor)}[Donor]_0[MP]_0 \quad (1)$$

where $[Donor]_0$ and $[MP]_0$ correspond to the initial donor and porphyrin concentrations. For those cases where the donor first decomposes to yield azanone and then reacts with the porphyrin, $k_{on(HNO)}$ was determined from the corresponding v_{on} vs HNO concentration plots (see Results section for a clear example), corresponding to the following reaction rate law

$$v_{on} = k_{on(HNO)}[HNO]_{ss}[MP]_0 \quad (2)$$

where $[MP]_0$ corresponds to the initial porphyrin concentration and $[HNO]_{ss}$ is the azanone *steady-state* solution concentration corresponding to each initial donor concentration estimated as in previous works from our groups.[17,41] Assuming steady state conditions, HNO producing (donor decomposition) and consuming reactions (dimerization, formation of the nitrosylporphyrin) rates must be equal. Donor decomposition and HNO dimerization rate constants are known, and the nitrosylporphyrin formation rate is measured in each case, allowing one to compute/estimate $[HNO]_{ss}$ according to the following equation

$$[HNO]_{ss} = \sqrt{\frac{k_d[Donor]_0}{2k_h}} \quad (3)$$

where $[Donor]_0$ corresponds to the initial donor concentration, k_d is the spontaneous donor decomposition rate constant, and k_h the azanone dimerization rate constant. It is possible that at pH 10 there is

dx.doi.org/10.1021/ic5007082 | Inorg. Chem. 2014, 53, 7351−7360

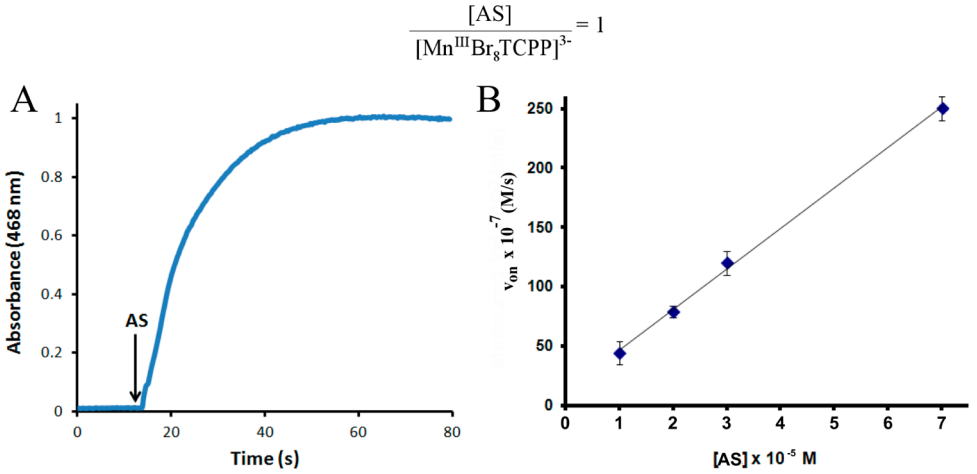

Figure 1. (A) Absorbance λ_{max} = 468 nm (corresponding to peak position of the nitrosyl complex) vs time plot for reaction of $[Mn^{III}Br_8TCPP]^{3-}$ 1 × 10^{-5} M with AS 1 × 10^{-5} M in phosphate buffer 0.1 M at 25 °C. (B) Initial rate (v_{on}) vs initial AS concentration plot for the corresponding reaction.

some contribution of $^3NO^-$ to the reaction rate. However, the fact that almost the same bimolecular rate constant is obtained for all porphyrins regardless of the pH and the HNO donor strongly suggests that if $^3NO^-$ contributes to the kinetics, either it reacts with a similar rate as HNO or its contribution is minor.

Electrochemical Detection of HNO. To determine azanone concentrations using our previously developed HNO-sensitive electrode,[41,42] the current response was measured after addition of the donor (1 × 10^{-5} M) to the porphyrin solutions (1 × 10^{-5} M) in an electrochemical cell. All experiments were performed at 25 °C in 0.1 M KNO_3 containing 10^{-4} M EDTA to avoid interferences or undesired reactions by Cu^{II} or other divalent cations. Milli-Q-grade water was used in all experiments; nitrogen and argon of high purity were used for all experiments. Amperometric measurements were carried out with a TEQ 03 potentiostat using a three-electrode system, consisting of platinum counter electrodes, Ag/AgCl as the reference, and the modified electrode as working electrode.

Computational Methods. All DFT calculations performed in this work were carried out using the Gaussian 98 software package.[29] All involved species were optimized at the B3LYP level using 6-31 G(d,p) for all atoms using water (polarizable continuum model, PCM) in order to take into account solvation effects. HNO donors (TSHA and AS) were studied in different protonation and oxidation states. For calculations involving metalloporphyrins, a simplified side chain lacking model Mn(III)/Fe(III) porphyrin was used. $M^{III}P$-coordinated complexes were computed in different electronic spin states (singlet, triplet, and quintuplet for Mn and doublet, quartet, and sextet for Fe) and with different possible donor (−N or −O linked) coordination states. Similar methodology has been successfully used to study both AS[43] and TSHA[44] decomposition as well as their potential interaction with metal complexes.[17]

RESULTS

The results are organized as follows: first, we show the UV−vis spectral changes for reaction of all porphyrins with azanone donors. Second, for each case we determine the reaction kinetics and the corresponding rate constants. Third, we use an amperometric-selective HNO sensor to test the production of HNO (or not) and thus confirm the proposed reaction mechanism. Last, we present results concerning DFT-based ab initio calculations on the reaction mechanism underlying porphyrin-accelerated donor decomposition.

1. UV−Vis Characterization of the Reactions of Mn/Fe Porphyrins with AS and TSHA. In order to study the mechanism of HNO donor reactions with metalloporphyrins, we determined the reactivity and kinetics of both AS and TSHA with the following porphyrins $[Mn^{III}Br_8TCPP]^{3-}$, $[Mn^{III}TCPP]^{3-}$, $[Mn^{III}Br_8TSPP]^{3-}$, $[Mn^{III}HematoP]^{-}$, $[Mn^{III}T(TriMA)P]^{5+}$, and $[Mn^{III}T\text{-}2\text{-}PyP]^{+}$, which together with those characterized in our previous works $[Mn^{III}TE\text{-}2\text{-}PyP]^{5+}$, $[Mn^{III}TSPP]^{3-}$, $[Mn^{III}ProtoP]^{-}$, $[(OH)Fe^{III}TE\text{-}2\text{-}PyP]^{4+}$, and $[(OH)Fe^{III}TSPP]^{4-}$ represent a comprehensive and diverse set. The choice of porphyrins is aimed to cover a complete set of peripheral charge (positive or negative) and reduction potential ($E_{1/2} > 0$, oxidizing, and $E_{1/2} < 0$, reducing) characteristics, as shown in Scheme 2. In other words, the term "oxidizing" refers to the electron-deficient porphyrins, which are eager to accept electrons and oxidize a target, while "reducing" refers to electron-rich porphyrins. We thus classify (or refer to) the porphyrins in four groups, which are positive oxidizing (PO), positive reducing (PR), negative oxidizing (NegO), and negative reducing (NegR).

For the following analysis we will use as examples $[Mn^{III}Br_8TCPP]^{3-}$ and $[Mn^{III}TCPP]^{3-}$ which differ in the presence/absence of eight bromine atoms in the corresponding beta carbons of the pyrrolic ring and thus have significantly different reduction potentials but bear the same peripheral negative charge. Figure 1A shows the spectral changes for reaction of $[Mn^{III}Br_8TCPP]^{3-}$ (a negative-oxidizing porphyrin) with AS in a 1:1 stoichiometric ratio. The reaction shows the typical behavior, according to our previous observations[17] for a reaction occurring through a *suspected* direct donor−porphyrin interaction, since it is fast (half-life of less than 5 s) and requires only a slight excess of donor to obtain a 100% yield of nitrosyl product. Another relevant observation is that in all cases only $Mn^{III}P$ and $\{MnNO\}^6$ were detected, suggesting that the hypothetical complex $Mn^{III}P$−(Donor), if formed, does so in an insignificant amount.

Figure SI1B, Supporting Information, shows the spectral changes for reaction of $[Mn^{III}TCPP]^{3-}$ (a negative-reducing porphyrin) with AS in 1:100 stoichiometric ratio. The reaction shows, on the contrary, the typical behavior for a reaction occurring through a pathway involving donor decomposition and subsequent HNO trapping by the porphyrin. It is quite slow (half-life of ca. 120 min) and requires over 100 times excess of donor to yield complete nitrosyl product formation. As expected and analyzed in our previous work, most of the

dx.doi.org/10.1021/ic5007082 | Inorg. Chem. 2014, 53, 7351−7360

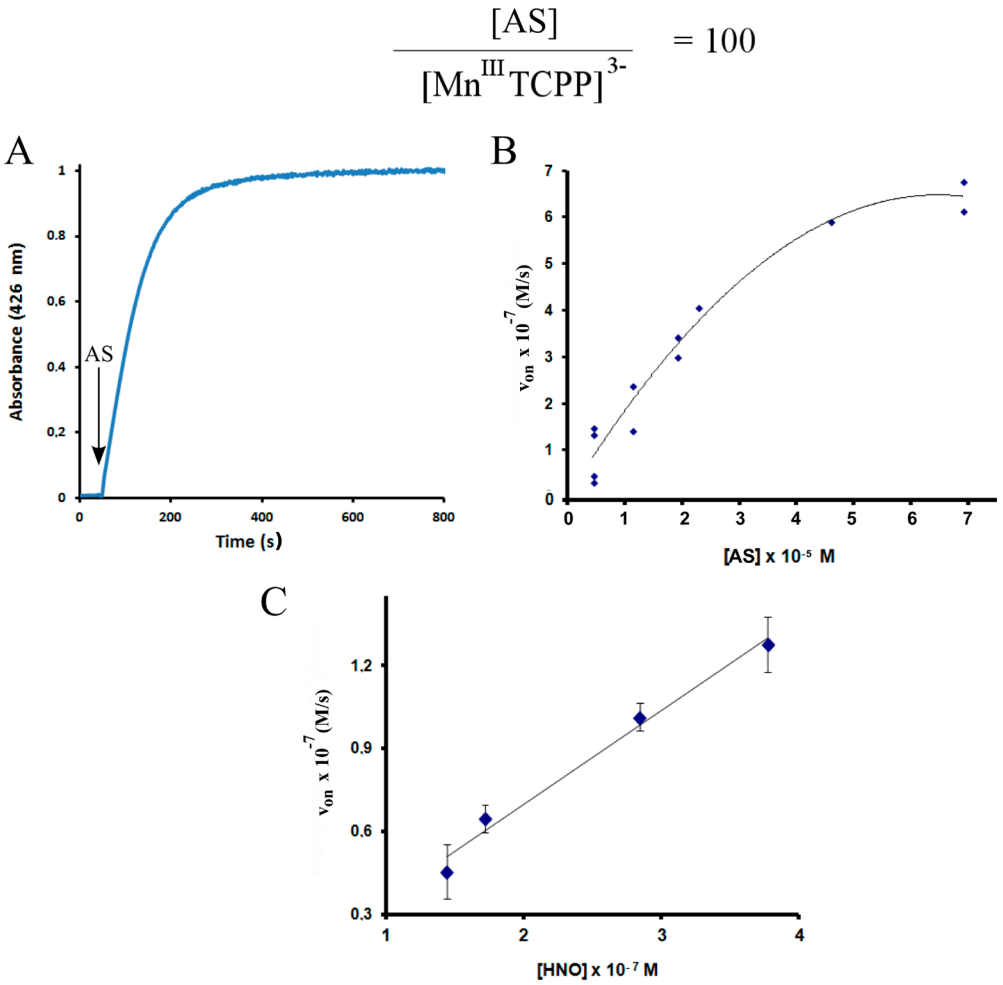

Figure 2. (A) Absorbance (λ_{max} = 426 nm, corresponding to peak position of the nitrosyl complex) vs time plot for reaction of $[Mn^{III}TCPP]^{3-}$ 1×10^{-5} M with AS 1×10^{-3} M in phosphate buffer 0.1 M at 25 °C. (B) Initial rate (v_{on}) vs initial AS concentration plot for the corresponding reaction. (C) Initial rate (v_{on}) vs [HNO] concentration plot for the corresponding reaction.

produced HNO that does not react with the porphyrin ends up as N_2O.[17,23,28]

Similar results as those shown in Figures SI1A or SI1B, Supporting Information, were obtained for all studied porphyrins and also using TSHA as the azanone source (corresponding spectral changes for all cases are shown in the Supporting Information). The most striking feature revealed by the spectral changes, besides the difference in proposed mechanisms depending on the oxidizing or reducing properties of the porphyrins (see below), concerns the magnitude of the spectral changes, which are much larger (up to 30 nm in the Soret band) for Mn–porphyrins in all cases, when compared to Fe–Porphyrins, where the change in the Soret band position is small (ca. 2 nm). This result is in agreement with previous observations from our group.[17]

2. Kinetic Analysis of the Reactions. We now turn our attention to the kinetic analysis. In all cases we determined either $k_{on(Donor)}$ or $k_{on(HNO)}$ using the corresponding analysis scheme presented in the Materials and Methods section. As an example of the reactions where direct donor–porphyrin interaction (or accelerated decomposition) is proposed (steps 1 and 2 of Scheme 1), in Figure 1A we show the $[Mn^{II}NO]_{Abs}$ vs time plot for reaction of AS with $[Mn^{III}Br_8TCPP]^{3-}$. From this plot, for different initial donor:porphyrin ratios the initial rate v_{on} can be determined and used to build the corresponding v_{on} vs [AS] plot, as shown in Figure 2B, from which the corresponding $k_{on(Donor)}$ is determined using eq 1. It is important to note that for the whole range of porphyrins to donor ratios (1:1–1:10) the plot is linear, consistent with a direct porphyrin–donor interaction mechanism (see below).

Figure 2A shows the absorbance of the nitrosyl product vs time plot for reaction of $[Mn^{III}TCPP]^{3-}$ with AS in 1:100 ratio, which we assume occurs through reactions 3 and 4 in Scheme 1. The plot, especially when compared to that in Figure 1A, shows that the nitrosyl product formation rate is slow (half-life of ca. 100 s compared to 5 s for Figure 1A). As for the previous case, from each plot with different initial donor:porphyrin ratios the product formation rates v_{on} were determined, and using eq 3 the corresponding azanone concentration was estimated. Both values were in turn used to build the corresponding v_{on} vs [HNO] plot, shown in Figure 2C, from which the corresponding rate constant $k_{on(HNO)}$ was obtained. Note that in this case, where the reaction involves spontaneous donor decomposition to yield azanone and then reacts with the porphyrin, the v_{on} vs initial donor concentration plot (Figure 1B) is not linear but displays an inverse square shape, due to the corresponding relation between initial donor and steady state azanone concentration described by eq 1 in the Materials and Methods section.

dx.doi.org/10.1021/ic5007082 | Inorg. Chem. 2014, 53, 7351–7360

Table 1. Association Rate Constants for Reactions of Mn(III)/Fe(III) Porphyrins with the Azanone Donors AS and TSHA

porphyrin	$E_{1/2}$ $Mn^{III/II}$ vs NHE (mV)[a]	porphyrin type	$k_{on(donor)} \times 10^{-3}$ (M^{-1} s^{-1}) AS pH 7	$k_{on(donor)} \times 10^{-3}$ (M^{-1} s^{-1}) TSHA pH 10	$k_{on(HNO)} \times 10^{-3}$ (M^{-1} s^{-1}) AS pH 7	$k_{on(HNO)} \times 10^{-3}$ (M^{-1} s^{-1}) TSHA pH 10	ref
$[Mn^{III}TE\text{-}2\text{-}PyP]^{5+}$	+228	PO	12 ± 1	10.0 ± 0.5			17
$[Mn^{III}Br_8TCPP]^{3-}$	+ 213	NegO	3.3 ± 0.3	4.4 ± 0.5			TW[c]
$[(OH)Fe^{III}TE\text{-}2\text{-}PyP]^{4+}$	+ 211	PO	5.8	11			28
$[Mn^{III}Br_8TSPP]^{3-}$	+ 209	NegO	3.7 ± 0.3	3.9 ± 0.2			TW[c]
$[(OH)Fe^{III}TSPP]^{4-}$	−100[b]	NegO	5×10^{-4}		1000 ± 40		45
$[Mn^{III}T(TriMA)P)]^{5+}$	−100	PR	$5.4 \pm 0.2 \times 10^{-2}$		110 ± 30		TW[c]
$[Mn^{III}TSPP]^{3-}$	−160	NegR			40	90	17
$[Mn^{III}TCPP]^{3-}$	−194	NegR			290 ± 50	160 ± 40	TW[c]
$[Mn^{III}ProtoP]^{-}$	−200	NegR			428 ± 4	186 ± 7	46
$[Mn^{III}HematoP]^{-}$	−230	NegR			160 ± 30	200 ± 50	TW[c]
$[Mn^{III}T\text{-}2\text{-}PyP]^{+}$	−280	PR			210 ± 40		TW[c]
$[Fe^{III}MP11]^{3-}$	−360	NegR			64	31	28

[a]Reduction potentials were measured at pH 7.8 in 0.05 M phosphate buffer, 0.1 M NaCl, with porphyrin concentration of 0.5 mM or were taken from ref 30. [b]$E_{1/2}$ of +23 mV vs NHE relates to aqua species; $E_{1/2}$ for $[(OH)FeTSPP]^{4-}$ has not be determined but is likely at least 100 mV more negative. [c]This work.

The same analysis was performed for all porphyrins and both azanone donors (TSHA and AS); the resulting donor or HNO association rate constants together with previously obtained rate constants for other cases are presented in Table 1.

The results presented in Table 1 show some clear trends. The first is that for all Mn porphyrins very similar $k_{on(HNO)}$ values are obtained with either AS or TSHA. The values are in the range from 3×10^4 to 5×10^5 M^{-1} s^{-1}, which is slightly slower than those observed for NO binding to ferric porphyrins (see below for a longer discussion on the subject). The $k_{on(Donor)}$ rate constant also shows a narrow distribution of values from 3×10^3 to 1×10^4 M^{-1} s^{-1} and similar rate constants for both donors AS and TSHA. The most interesting observation, however, is that instead of the previously observed trend[17] where positively charged Mn porphyrins showed catalytic donor decomposition and negative charged did not, when considering also the reduction potential it becomes clear that those Mn−porphyrins with positive reduction potential (>100 mV) promote donor decomposition despite their peripheral charge (i.e., being positively or negatively charged). On the other hand, those metalloporhyrins with a negative reduction potential (<160 mV) trap free HNO produced by decomposition of the donor. There is, however, a minor effect of the peripheral charges in the reaction with the dianionic AS donor, which is evident when comparing $[Mn^{III}Br_8TCPP]^{3-}$ or $[Mn^{III}Br_8TSPP]^{3-}$ with $[Mn^{III}TE\text{-}2\text{-}PyP]^{5+}$. Although in all three cases $E_{1/2}$ has a similar value, the positively charged porphyrin has a $k_{on(Donor)}$ 3.5 times higher than the other two species.

As shown by the data, there is a clear gap in the reduction potential between those Mn−porphyrins which accelerate donor decomposition and those which react with free HNO. However, what is most interesting is that in both cases displaying intermediate reduction potentials, i.e., in the "twilight zone", $[(OH)Fe^{III}TSPP]^{4-}$ and $[Mn^{III}T(TriMAP)]^{5+}$ with $E_{1/2}$ values of +23 and −100 mV, respectively, kinetic analysis with any of the two proposed mechanisms does not yield good results, since the obtained values for $k_{on(Donor)}$ or $k_{on(HNO)}$ are at odds with other cases. However, using a kinetic model that enables both processes to be operative allows determination of both rate constants simultaneously yielding $k_{on(HNO)}$ values which are similar to those obtained for the other porphyrins and, as expected, values for $k_{on(Donor)}$ which are significantly lower than those observed for the oxidizing porphyrins. Thus, it is clear that these porphyrins displaying intermediate reduction potentials have a smaller catalyzing efficiency for decomposition of the donor.

3. Electrochemical Assessment of HNO Concentration during Accelerated and Direct Reactions. In order to have additional evidence showing that oxidizing porphyrins accelerate donor decomposition through a direct interaction and thus there is no reaction with free HNO, while reducing porphyrins trap free HNO derived from spontaneous donor decomposition, we measured the instantaneous HNO concentration during the reaction time course using our recently developed, time-resolved selective HNO electrode.[41,42] Figure 3 shows the time-dependent electrochemical signal (which is proportional to [HNO]) upon addition of AS in the presence of an oxidizing porphyrin ($[Mn^{III}Br_8TCPP]^{3-}$, 1×10^{-5} M), a reducing porphyrin ($[Mn^{III}TCPP]^{3-}$, 1×10^{-5} M), and plain buffer solution. In all cases AS concentrations were kept constant at 1×10^{-5} M. The figure clearly shows that in plain buffer, after addition of AS, a fast peak signal is seen corresponding to the initial HNO produced by the donor

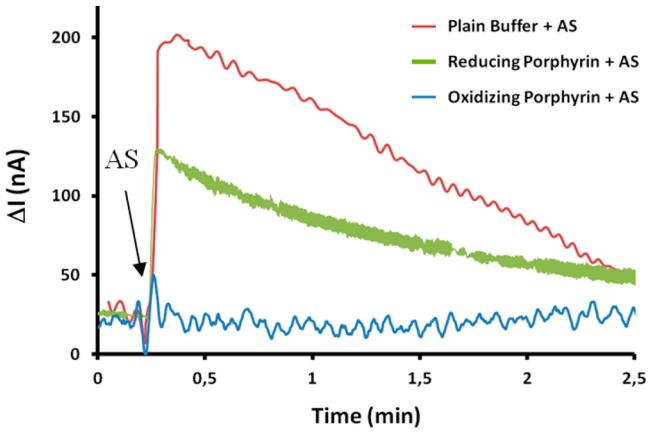

Figure 3. Time-dependent electrochemical signal upon addition of AS (arrow) in the presence of an oxidizing porphyrin ($[Mn^{III}Br_8TCPP]^{3-}$, 1×10^{-5} M, blue), a reducing porphyrin ($[Mn^{III}TCPP]^{3-}$, 1×10^{-5} M, green) and plain buffer solution (red). AS concentrations were 1×10^{-5} M in all cases.

dx.doi.org/10.1021/ic5007082 | Inorg. Chem. 2014, 53, 7351−7360

Scheme 3. Reactions Concerning AS[a]

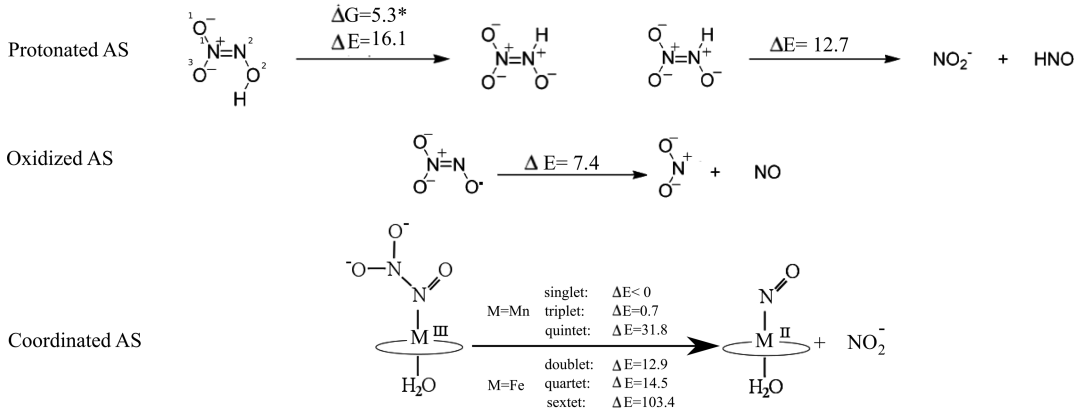

[a]Energy values are reported in kcal/mol; ref 35.

decomposition that subsequently levels off and then decays slowly as a result of the equilibrium between spontaneous donor decomposition and HNO dimerization (see ref 33 for a longer discussion of the signal plot shape). The presence of an oxidizing porphyrin completely abolishes the HNO signal, as expected for a direct donor−porphyrin interaction (the detection limit of the sensor is ca. 1 nA (~1 nM)), thus verifying our hypothesis derived from the kinetic data. Also interesting is the fact that in the presence of a reducing porphyrin the HNO signal is observed (since spontaneous donor decomposition occurs) but the profile is different from that obtained in plain buffer. Kinetic analysis of the trace allows, as shown in our previous work,[41] determination of the HNO to porphyrin bimolecular rate constant (see Supporting Information for details), which as expected yields the same value 2×10^5 M^{-1} s^{-1}, obtained by the previously described spectroscopic method.

4. DFT Calculations Related to HNO Production by Oxidized AS and TSHA. In order to get deeper insight into the mechanism of donor decomposition accelerated by metalloporphyrin, we performed ab initio calculations of key reaction intermediates and energetics. Computational methods have been previously used to study both AS[43,47] and TSHA[44] decomposition mechanisms to yield azanone and NO.[2] Studies on trioxodinitrate show that in the pH decomposition range pH = 4−8 an equilibrium between the N2 and O2 atoms protonated forms exists (see Scheme 3 for atom numbering) and that the N2 protonated atom corresponding to AS has a weaker N−N bond that can be spontaneously broken to yield HNO and nitrite. The N2 atom protonated state is estimated to lie ca. 13 kcal/mol higher in energy and 5.3 kcal/mol in free energy compared to the most stable O2 atom protonated state. The energy barrier required to break the N−N bond was estimated to be about 7.8 kcal/mol with B3LYP and the PCM model,[43] while the free energy barrier in explicit water was estimated to be 4.8 kcal/mol with B3LYP (6.5 kcal/mol with MP2).[47] Previous work from our group showed that if AS coordinates to the Mn−porphyrin through the N2 atom it spontaneously yields the nitrosyl porphyrin and nitrite (i.e., coordination accelerates AS decomposition).[17] On the basis of the present kinetic data which shows that those porphyrins with a positive (>+100 mV) reduction potential accelerate AS decomposition, we decided to test using DFT whether AS oxidation may also induce its decomposition and analyze its coordination effects further (all results are summarized in Scheme 3). Our results for AS show that metal coordination of the N2 atom is more favorable than for the O2 atom by 11.6 kcal/mol for FeP and 31.5 kcal/mol for MnP. Once coordinated, in the singlet state, MnP−AS spontaneously yields MnPNO and NO_2^-, as previously observed. For the iron case, N−N bond breaking requires similar energy as for the noncoordinated AS protonated at the N2 atom. Lastly, analysis of the porphyrin−AS adducts reveals that spin state energy ordering is singlet < triplet < quintet (for d^4 $Mn^{III}P$) or doublet < quartet < sextet (for d^5 $Fe^{III}P$). The singlet and doublet ground states for the Mn(III) and Fe(III) adducts, respectively, indicate a low-spin species of maximum electron pairing, consistent with coordination of strong field, N-bonded nitroso-type ligands,[48,49] (i.e., via N2). It is worth noting that replacement of the electron-withdrawing O_2N- moiety of AS by an electron-donating R_2N- moiety (R = alkyl) yields nitrosamines (R_2N-NO) that coordinate to Fe(III) porphyrins to give rise to O-bound, high-spin d^5, sextet adducts.[50,51] The preferred N coordination is therefore in contrast with that observed for nitrosamines,[52] where O coordination is favored. Remarkably, coordinated nitrosamines also end up as MNO compounds after a while.

Interestingly, oxidation of noncoordinated AS yields a stable $N_2O_3^{-}$* radical anion, which conjugated acid is expected to display a low pK_a and thus in the physiological range the radical anion is expected to be negatively charged. Analysis of its electronic structure shows that in the AS oxidized radical the N−N bond becomes weaker (the N−N distance is enlarged by ca. 0.15 Å with respect to any AS tautomer) and the unpaired spin density is almost completely localized (0.71 *e*) on the NO. Furthermore, breaking of the N−N bond to yield NO_2^- and NO is 7.3 kcal/mol lower for the oxidized AS radical when compared to AS protonated on the N2 atom.

Concerning TSHA and similar compounds, the key $-SO_2NHOH$ moiety contains two proton-like hydrogen atoms: one on the N atom and the other on the O atom. TSHA decomposition to yield HNO is produced in basic media, and the rate and pH range observed suggests S−N bond breaking of the singly protonated species as the key step.[44] Computational studies on the sulfohydroxamic acid moiety show that, similarly to what is observed for AS, protonation on the O atom is favored by about 10 kcal/mol, while S−N bond breaking is easier for the N protonated state, displaying a bond strength of 14.5 kcal/mol at the B3LYP/PCM level of theory.[44] As for the AS case, TSHA-accelerated decomposition can occur

dx.doi.org/10.1021/ic5007082 | Inorg. Chem. 2014, 53, 7351−7360

Scheme 4. Reactions Concerning TSHA[a]

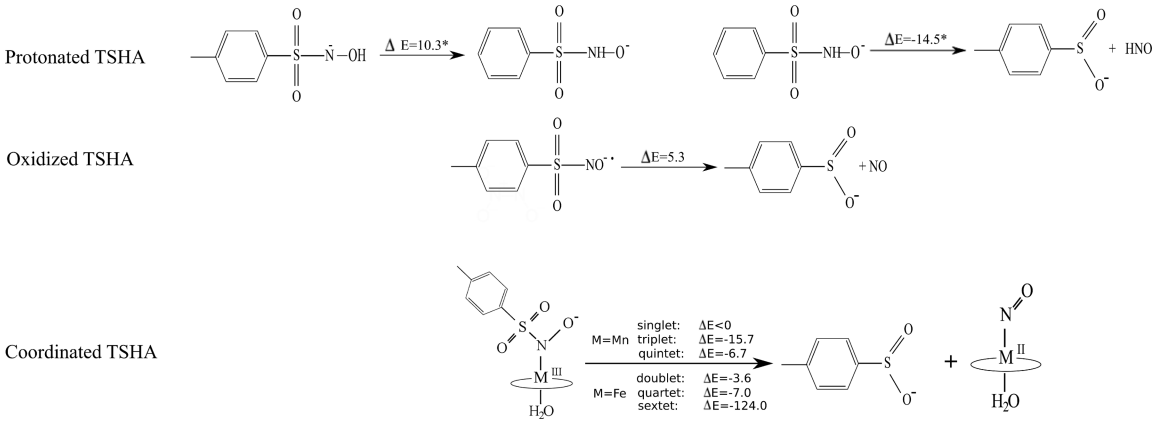

[a]Energy values are reported in kcal/mol.[36]

either through direct coordination with the porphyrin or through and outer-sphere electron transfer process that results in an oxidized form of the sulfohydroxamic acid moiety. Coordination of the N atom to the metalloporphyrin is also favored in TSHA (by 44.0 kcal/mol for MnP) and, as in AS, MnP−TSHA spontaneously yields MnPNO. Oxidation of TSHA yields a stable radical species whose electronic structure shows that the unpaired spin density is almost exclusively localized on the NO, and again and similarly to what was observed for AS, breaking of the S−N bond is lowered by 9.2 kcal/mol (all results are summarized in Scheme 4).

Taken together, these results show common aspects of metal coordination and/or oxidative promotion of both AS and TSHA donors decomposition. Coordination preference for the N atom for both donors (in contrast to protonation which is favored at the oxygen atom of the leaving HNO group) and the resulting induced N(S)−N bond breakage to yield stable nitrosyl nicely accounts for decomposition promoted by metalloporphyrin. Furthermore, oxidation of both donors results in radical species that display weaker N(S)−N bond strengths and yield NO, avoiding the need for protonation of the N atom.

DISCUSSION

Since the founding observation of Farmer and co-workers over 10 years ago of a stable Mb−HNO adduct, closely followed by our own studies of the reactivity of HNO with Fe^{III} and Mn^{III} porphyrins, intensive research has been performed on HNO and its reactivity at its donors, especially with metalloproteins and organometallic and biomimetic complexes.[1,20,21,53,54] In the present work, we thoroughly studied the reaction mechanism of two commonly used azanone donors: trioxodinitrate (AS) and toluensulfohydroxamic acid (TSHA), with a series of Mn^{III} and Fe^{III} water-soluble porphyrins which cover a wide range of peripheral charges and reduction potential. Our main observation is related to the fact that metalloporphyrins can react either directly with the donor, catalyzing its decomposition, or alternatively trap the free HNO produced by spontaneous decomposition of the donor.

Kinetic studies of the direct reaction cases allows determination of the bimolecular rate constants for reaction of "free and soluble" HNO (whose presence is strongly supported by the electrode measurements) with Mn^{III} and Fe^{III} porphyrins, yielding biomolecular rate constants values in the range from 4×10^4 to 4×10^5 M^{-1} s^{-1}. The obtained values can be compared to those obtained for HNO, as well as NO, binding to ferrous and ferric heme−proteins, as well as other heme models, as shown in Table 2. The first observation can be drawn from the comparison of the HNO binding rate obtained for Mn^{III} and Fe^{III} porphyrins which can be thought of as tetracoordinated (4c) (i.e., they bear no strong axial ligand coordinated to the metal), when compared to Fe^{III}MP11 (a pentacoordinated (5c) protein free model, due to coordination of a histidine), and the His pentacoordinated proteins such as Mb, MnMb, or catalase, and the His-Met hexacoordinated (6c) Cyt-c. Interestingly, all determined rate constants fall in the same range from 1×10^4 to 1×10^5 M^{-1} s^{-1}, thus suggesting a minor role for the protein matrix as well as the axial endogenous ligands. These values are very similar and only slightly smaller than those reported for NO binding to Mn^{III} and Fe^{III} porphyrins, while they are significantly smaller when compared to NO binding to ferrous porphyrins or heme−proteins, with rate constants greater than 1×10^7 M^{-1} s^{-1}. A possible explanation for the homogeneous HNO binding rate constant observed, as proposed by Lorkovic and Ford for NO binding to ferric hemes,[14,55] lies in the fact that actually Fe^{III} porphyrins as well as heme−proteins are not really 4c or 5c but always 6c due to the presence of coordinating waters or hydroxide ions to the axial sites of the metal center. Release of this ligand is possibly rate limiting and sets a limit to the HNO binding rate constant. Under all pH conditions studied, Fe

Table 2. Kinetic Rate Constants for Reactions of HNO and NO with Ferrous and Ferric Heme−Proteins and Heme Models

target	$E_{1/2}$ vs NHE (mV)	reactant	k_{on} (M^{-1} s^{-1})	ref
Fe^{III}MP11	−360	HNO	3.1×10^4	28
		NO	1.1×10^6	60
$[(OH)Fe^{III}TSPP]^{4-}$	+23	NO	4.5×10^5	45
$[Fe^{II}TSPP]^{-}$	−300	NO	1.5×10^9	45
Cyt-c(Fe^{III})	+250	HNO	4×10^4	30
catalase(Fe^{III})	−226	HNO	3×10^5	30
metMb(Fe^{III})	+120	HNO	8×10^5	30
Mb(Mn^{III})	−320	HNO	3.4×10^5	46
Mb(Fe^{II})	−430	HNO	1.4×10^4	54
		NO	2.0×10^7	61
O_2		HNO	3×10^3	30

dx.doi.org/10.1021/ic5007082 | Inorg. Chem. 2014, 53, 7351−7360

porphyrins exist as monohydroxo species. Replacement of one aqua with a hydroxo ligand results in stabilization of Fe in +3 oxidation state, which is reflected in a shift in reduction potential from +380 to +211 mV vs NHE.[28,51] Thus, Fe and Mn analogs, $[(OH)FeTE\text{-}2\text{-}PyP]^{4+}$ and $[MnTE\text{-}2\text{-}PyP]^{5+}$, have nearly identical $E_{1/2}$ values, which in turn results in near identical rate constants, $k_{on(Donor)}$ (Table 1).

The obtained bimolecular HNO reaction rate with metal porphyrins/proteins can also be considered in the context of other reactants like O_2, NO, or thiols.[56−59] The reaction is faster by 1−2 orders of magnitude compared to reaction of azanone with oxygen; thus, even for aerobic and especially for physiological compatible low oxygen (anoxic) conditions, metal−porphyrins can be used as efficient HNO traps and reaction of HNO with ferric heme proteins is expected to occur. Reaction of HNO with NO is, on the other hand, significantly faster, with values close to that of HNO dimerization; thus, in the presence of nitric oxide, NO will consume the azanone before it can be trapped. This observation has important implications, since it shows that HNO detection using metalloporphyrins will be less efficient when NO is present at relatively high concentrations.

Our results also have implications in relation to the studies of donor decomposition mechanisms to yield HNO. The donors used in the present work (AS and TSHA) can be viewed as representative members of NONOates and sulfohydroxamic acid groups of donors, respectively. First, from the general perspective of how these chemical entities release HNO, it is noteworthy that one-electron oxidation results in a significant enhancement of NO release by weakening of the $N-N_{NO}$ and $S-N_{NO}$ bonds in AS and TSHA, respectively. Second, the fact that the oxidative process and direct coordination of the donor to electron-avid metal centers promotes (or accelerates) their decomposition to yield HNO strongly suggests that care should be taken when interpreting kinetic and mechanistic results concerning azanone donors reactivity and assuming that the reactant is really free HNO. Our results show that both careful kinetic model analysis as well as direct and independent determination of azanone concentrations along the reaction can be used to assess whether a genuine HNO reaction is actually happening or if the donor is directly reacting with the studied compound.

Lastly, our results provide a rationale for selecting adequate Mn−porphyrins to be used in HNO trapping, detection, and quantification experiments. According to the proposed mechanisms, the reducing Mn−porphyrins offer the best choice, since they avoid direct interaction with the donor and can efficiently trap soluble azanone. However, it is also important to take into consideration the stability of the resulting nitrosyl complex. As shown in our previous works,[17] $\{MnPNO\}^7$ complex can be readily oxidized by molecular oxygen and thus lead to an underestimation of the $\{MnPNO\}^7$ concentration and therefore the HNO presence. This can be partially avoided by protecting the $Mn^{III}P$ in a protein matrix,[46] like that of Mb. $Mn^{III}Mb$ displays a negative reduction potential (−320 mV), its reaction with azanone donors is compatible with no direct interaction, and it traps the soluble HNO with a fast 3.2×10^5 M^{-1} s^{-1} bimolecular rate constant.

CONCLUSIONS

In the present work we have shown that (i) two mechanisms account for the reaction of metalloporphyrins with azanone donors. The first occurs in the presence of oxidizing porphyrins ($E_{1/2}$ > 100 mV), which accelerate oxidative decomposition of the donor. The second, in the case of reducing porphyrins ($E_{1/2}$ < −160 mV), requires spontaneous decomposition of the donor to yield free HNO, which subsequently reacts with the porphyrins. (ii) The bimolecular reaction rate constants for HNO binding to $M^{III}P$ is in the range from 4×10^4 to 4×10^5 M^{-1} s^{-1} (M = Fe,Mn).

ASSOCIATED CONTENT

Supporting Information

Spectral changes for selected reactions, absorption bands and molar absorptivities, comparison of the reactions for two porphyrins, and a kinetic model. This material is available free of charge via the Internet at http://pubs.acs.org.

AUTHOR INFORMATION

Corresponding Author

*Phone: (5411)-4576-3378 ext. 116. Fax: (5411)-4576-3341. E-mail: doctorovich@qi.fcen.uba.ar.

Notes

The authors declare no competing financial interest.

ACKNOWLEDGMENTS

This work was financially supported by UBA (UBACYT W583 and 2010-12), ANPCyT (PICT 2010-2649 and 2010-416), CONICET (PIP1207 and 112-201001-00125), and the Bunge y Born Foundation. D.E.B., M.A.M., and F.A.D. are members of CONICET.

REFERENCES

(1) Doctorovich, F.; Bikiel, D.; Pellegrino, J.; Suárez, S. A.; Larsen, A.; Martí, M. A. *Coord. Chem. Rev.* **2011**, *255*, 2764−2784.
(2) Miranda, K. *Coord. Chem. Rev.* **2005**, *249*, 433−455.
(3) Shafirovich, V.; Lymar, S. V. *J. Am. Chem. Soc.* **2003**, *125*, 6547−52.
(4) Paolocci, N.; Jackson, M. I.; Lopez, B. E.; Miranda, K.; Tocchetti, C. G.; Wink, D. A.; Hobbs, A. J.; Fukuto, J. M. *Pharmacol. Ther.* **2007**, *113*, 442−58.
(5) Wink, D. A.; Miranda, K. M.; Katori, T.; Mancardi, D.; Thomas, D. D.; Ridnour, L.; Espey, M. G.; Feelisch, M.; Colton, C. A.; Fukuto, J. M.; Pagliaro, P.; Kass, D. A.; Paolocci, N. *Am. J. Physiol. Heart Circ. Physiol.* **2003**, *285*, H2264−76.
(6) Heinecke, J. L.; Khin, C.; Pereira, J. C. M.; Suárez, S. A.; Iretskii, A. V.; Doctorovich, F.; Ford, P. C. *J. Am. Chem. Soc.* **2013**, *135*, 4007−17.
(7) Simonaitis, R. *J. Phys. Chem.* **1963**, *67*, 2227−2228.
(8) Clyne, M. A. A.; Thrush, B. A. *Trans. Faraday Soc.* **1961**, *57*, 1305−1314.
(9) Strausz, O. P.; Gunning, H. E. *Trans. Faraday Soc.* **1964**, *60*, 347.
(10) Wright, A. M.; Wu, G.; Hayton, T. W. *J. Am. Chem. Soc.* **2012**, *134*, 9930−3.
(11) Zheng, S.; Berto, T. C.; Dahl, E. W.; Hoffman, M. B.; Speelman, A. L.; Lehnert, N. *J. Am. Chem. Soc.* **2013**, *135*, 4902−5.
(12) Speelman, A. L.; Lehnert, N. *Acc. Chem. Res.* **2014**, *47*, 1106−16.
(13) Sabat, J.; Egawa, T.; Lu, C.; Stuehr, D. J.; Gerfen, G. J.; Rousseau, D. L.; Yeh, S.-R. *J. Biol. Chem.* **2013**, *288*, 6095−106.
(14) Ford, P. C. P. C.; Lorkovic, I. M. I. M. *Chem. Rev.* **2002**, *102*, 993−1018.
(15) Franke, A.; Suzuki, N.; Higuchi, T.; Okuzono, K.; Eldik, R. Van; Chemistry, F. *World* **2005**, 5360−5375.
(16) Roncaroli, F.; Eldik, R. Van *J. Am. Chem. Soc.* **2006**, *128*, 8042−8053.
(17) Martí, M. a; Bari, S. E.; Estrin, D. A.; Doctorovich, F. *J. Am. Chem. Soc.* **2005**, *127*, 4680−4.
(18) Guillaud, G. *Coord. Chem. Rev.* **1998**, *178−180*, 1433−1484.

(19) Lehnert, N.; Scheidt, W. R.; Wolf, M. W. *Struct. & Bonding* **2014***154*155224.
(20) Farmer, P. J.; Sulc, F. *J. Inorg. Biochem.* **2005**, *99*, 166−84.
(21) Lin, R.; Farmer, P. J. *J. Am. Chem. Soc.* **2000**, *122*, 2393−2394.
(22) Immoos, C. E.; Sulc, F.; Farmer, P. J.; Czarnecki, K.; Bocian, D. F.; Levina, A.; Aitken, J. B.; Armstrong, R. S.; Lay, P. a *J. Am. Chem. Soc.* **2005**, *127*, 814−5.
(23) Bari, S. E.; Martí, M. A.; Amorebieta, V. T.; Estrin, D. A.; Doctorovich, F. *J. Am. Chem. Soc.* **2003**, *125*, 15272−3.
(24) Pellegrino, J.; Bari, S. E.; Bikiel, D. E.; Doctorovich, F. *J. Am. Chem. Soc.* **2010**, *132*, 989−95.
(25) Goodrich, L. E.; Roy, S.; Alp, E. E.; Zhao, J.; Hu, M. Y.; Lehnert, N. *Inorg. Chem.* **2013**, *52*, 7766−7780.
(26) Kurtikyan, T. S.; Gulyan, G. M.; Martirosyan, G. G.; Lim, M. D.; Ford, P. C. *J. Am. Chem. Soc.* **2005**, *127*, 6216−6224.
(27) Møller, J. K. S.; Skibsted, L. H. *Chemistry* **2004**, *10*, 2291−300.
(28) Suárez, S. A.; Martí, M. A.; De Biase, P. M.; Estrin, D. a.; Bari, S. E.; Doctorovich, F. *Polyhedron* **2007**, *26*, 4673−4679.
(29) Spasojevic, I.; Batini-Haberle, I.; Fridovich, I. *Nitric Oxide* **2000**, *4*, 526−533.
(30) Miranda, K. M.; Paolocci, N.; Katori, T.; Thomas, D. D.; Ford, E.; Bartberger, M. D.; Espey, M. G.; Kass, D. A.; Feelisch, M.; Fukuto, J. M.; Wink, D. A. *Proc. Natl. Acad. Sci. U.S.A.* **2003**, *100*, 9196−201.
(31) Bonner, F. T.; Degani, H.; Akhtar, M. J. *J. Am. Chem. Soc.* **1981**, *103*, 3739−3742.
(32) Batinic-Haberle, I.; Spasojevic, I.; Hambright, P.; Benov, L.; Crumbliss, A. L.; Fridovich, I. *Inorg. Chem.* **1999**, *38*, 4011−4022.
(33) Ferrer-Sueta, G.; Hannibal, L.; Batinic-Haberle, I.; Radi, R. *Free Radical Biol. Med.* **2006**, *41*, 503−12.
(34) Batinic-Haberle, I.; Spasojevic, I.; Tse, H.; Tovmasyan, A.; St. Clair, D. K.; Vujaskovic, Z.; Dewhirst, M. D.; Piganelli, J. D. *Amino Acids* **2012**, *42*, 95−113.
(35) Rebouças, J. S.; Spasojević, I.; Batinić-Haberle, I. *J. Biol. Inorg. Chem.* **2008**, *13*, 289−302.
(36) Delmastro-Greenwood, M. M.; Votyakova, T.; Goetzman, E.; Marre, M. L.; Previte, D. M.; Tovmasyan, A.; Batinic-Haberle, I.; Trucco, M. M.; Piganelli, J. D. *Antioxid. Redox Signaling* **2013**, *19*, 1902−15.
(37) Batinic-Haberle, I.; Tovmasyan, A.; Spasojevic, I. *Bioinorg. React. Mech.* **2013**, *9*, 35−58.
(38) Seel, F.; Bliefert, C. *Z. Anorg. Allg. Chem.* **1972**, *394*, 187−196.
(39) Hughes, M.; Cammack, R. *Methods Enzymol.* **1999**, *301*, 279−287.
(40) Hughes, M. N.; Wimbledon, P. E. *J. Chem. Soc., Dalton Trans.* **1976**, *8*, 703−707.
(41) Suárez, S.; Bikiel, D.; Wetzler, D.; Martí, M. A.; Doctorovich, F. *Anal. Chem.* **2013**, *85*, 10262−10269.
(42) Suárez, S. A.; Fonticelli, M. H.; Rubert, A. a; de la Llave, E.; Scherlis, D.; Salvarezza, R. C.; Martí, M. a; Doctorovich, F. *Inorg. Chem.* **2010**, *49*, 6955−66.
(43) Dutton, A. S.; Fukuto, J. M.; Houk, K. N. *J. Am. Chem. Soc.* **2004**, *126*, 3795−800.
(44) Sirsalmath, K.; Suárez, S. A.; Bikiel, D. E.; Doctorovich, F. *J. Inorg. Biochem.* **2013**, *118*, 134−139.
(45) Laverman, L. E.; Ford, P. C. *J. Am. Chem. Soc.* **2001**, *123*, 11614−11622.
(46) Boron, I.; Suárez, S. A.; Doctorovich, F.; Martí, M. A.; Bari, S. E. *J. Inorg. Biochem.* **2011**, *105*, 1044 −1049.
(47) Torras, J.; Seabra, G.; Roitberg, A. *J. Chem. Theory* **2009**, *5*, 37−46.
(48) Liang, J.-L.; Huang, J.-S.; Zhou, Z.-Y.; Cheung, K. K.; Che, C.-M. *Chem.—Eur. J.* **2001**, *7*, 2306−2317.
(49) Crotti, C.; Sishta, C.; Pacheco, A.; James, B. R. *Inorg. Chim. Acta* **1988**, *141*, 13−15.
(50) Ti, G.-B.; Khan, M. A.; Richter-Addo, G. B. *Inorg. Chem.* **1996**, *35*, 3453−3554.
(51) Leitão, E. F. V.; Ventura, E.; Santana, O. L.; do Monte, S. A. *Int. J. Quantum Chem.* **2014**, DOI: 10.1002/qua.24595.
(52) Xu, N.; Goodrich, L. E.; Lehnert, N.; Powell, D. R.; Richter-Addo, G. B. *Inorg. Chem.* **2010**, *49*, 4405−19.
(53) Farmer, P.; Kumar, M.; Almaraz, E. *Comments Inorg. Chem.* **2010**, *31*, 130−143.
(54) Sulc, F.; Immoos, C. E.; Pervitsky, D.; Farmer, P. J. *J. Am. Chem. Soc.* **2004**, *126*, 1096−101.
(55) Lim, M. D.; Lorkovic, I. M.; Ford, P. C. *J. Inorg. Biochem.* **2005**, *99*, 151−165.
(56) Miranda, K. M. *Coord. Chem. Rev.* **2005**, *249*, 433−455.
(57) Bartberger, M. D.; Fukuto, J. M.; Houk, K. N. *Proc. Natl. Acad. Sci. U.S.A.* **2001**, *98*, 2194−8.
(58) Liochev, S. I.; Fridovich, I. *Free Radical Biol. Med.* **2003**, *34*, 1399−1404.
(59) Lymar, S. V.; Shafirovich, V.; Poskrebyshev, G. A. *Inorg. Chem.* **2005**, *44*, 5212−21.
(60) Sharma, V. S.; Isaacson, R. A.; John, M. E.; Waterman, M. R.; Chevion, M. *Biochemistry* **1983**, *22*, 3897−3902.
(61) Scott, E. E.; Gibson, Q. H.; Olson, J. S. *J. Biol. Chem.* **2001**, *276*, 5177−5188.